Effect of CO_2 on the Properties of AOT/Water/Isooctane Reverse Micelles by Fluorescence Study

Dongxia Liu, Jianling Zhang, Jiufeng Fan, Buxing Han,* and Jing Chen

Center for Molecular Science, Institute of Chemistry, The Chinese Academy of Sciences, Beijing 100080, People's Republic of China

Received: September 8, 2003; In Final Form: December 11, 2003

The effect of compressed CO_2 on the properties of sodium bis(2-ethylhexyl) sulfosuccinate/water/isooctane reverse micelles was investigated by steady-state and time-resolved fluorescence spectroscopic techniques. With the solvatochromic fluorescent probe 6-propionyl-2-(dimethylamino)-naphthalene, the steady-state fluorescence spectroscopy indicates a changed environment in multiple microregions of the reverse micelles with increasing CO_2 pressure. Quantitative estimates for the micropolarities of micellar cores at different pressures were carried out in terms of the empirical polarity parameter $E_T(30)$. The results show that $E_T(30)$ is gradually increased with the pressure. The emission of 8-anilino-1-naphthalenesulfonic acid indicates a reduced viscosity inside the micellar cores. Its reduced lifetime characterizes the dynamic property of solvent reorientation within micellar cores increases with the increasing CO_2 pressure.

1. Introduction

Reverse micelles are nanometer-sized droplets of polar solvent surrounded by a layer of surfactant molecules dispersed in a nonpolar or weakly polar solvent.[1−3] Sodium bis(2-ethylhexyl)-sulfosuccinate (AOT) is a widely used surfactant to form reverse micelles in nonpolar solvent.[4−7] Water is readily solubilized in the polar core of the reverse micelles to form a "water pool" characterized by water-to-surfactant molar ratio (w_0),[8−10] which has been extensively used as a novel microreactor for carrying out many kinds of chemical and biochemical reactions.[11−15] The properties of the enclosed water in the reverse micelles, which are different from those of bulk water, have been widely studied with various methods.[16−23]

Fluorescence spectroscopy is widely used to investigate properties of the reverse micelles due to their suitable time scale, noninvasive nature, and intrinsic sensitivity.[24−26] In fluorescence methods, the steady-state fluorescence spectroscopy is often employed to probe the average properties, like microviscosity, micropolarity, and rigidity within the water pool. For extremely fast processes, such as solvation, the time-resolved fluorescence is often used with extremely high sensitivity. In fluorescence studies, the use of fluorescent probes is attractive since the fluorescence characteristics (e.g., fluorescence intensity, excitation and emission wavelength maximum, lifetime, polarization, etc.) can reflect their microenvironment, thus improving the understanding of properties within local environment. For AOT/water/alkane systems, 6-propionyl-2-(dimethylamino)-naphthalene (Prodan) is a commonly used fluorescence probe because it distributes over all regions of the reverse micelles and gives a global picture of the reverse micelles. In addition, its ability to display appreciable shifts in the wavelength of maximum emission (λ_{em}^{max}) can characterize the environmental polarity.[27−29] 8-Anilino-1-naphthalenesulfonic acid (8,1-ANS) is also usually used in the reverse micellar systems. It is reported to partition into the aqueous micellar core[21] and probe the degree of motion of water inside the reverse micelles, which provides the information of microproperties and dynamic processes within reverse micelles.[30−32]

Supercritical (SC) or compressed carbon dioxide (CO_2) has recently received much attention because of its readily available, inexpensive, nontoxic, nonflammable, and environmentally benign characteristics.[33−36] One of the important applications of SC or compressed CO_2 is to precipitate solutes from solutions, which is known as the gas antisolvent (GAS) process.[37−39] In the GAS process, the properties of the organic solvents can be tuned continuously by changing the pressure of CO_2. More recently, we studied the effect of dissolved CO_2 in reverse micellar solutions on the solubilization of biomolecules (lysozyme and bovine serum albumin)[40,41] and different inorganic nanoparticles synthesized in the reverse micelles.[42−43] The results demonstrate that pure products can be recovered from the reverse micelles by controlling CO_2 pressure, while the surfactants remain in the organic-continuous phase. The combination of the reverse micelles and compressed CO_2 may provide a useful medium for different applications since the properties of the reverse micelles can be tuned by CO_2 pressure.

Understanding of the related fundamental knowledge is an interesting topic. In previous work, we studied the effect of compressed CO_2 on some properties of AOT/water/isooctane reverse micelles using synchrotron radiation small-angle X-ray scattering (SAXS),[44] Fourier transform infrared (FT-IR) and UV−vis spectra.[45] It was demonstrated that compressed CO_2 has considerable effect on the size of the reverse micelles and the pH, polarity, and ionic strength of the water cores in the reverse micelles. In this paper, we employed steady-state and time-resolved fluorescence techniques to characterize the fluorescence emission properties of Prodan and 8,1-ANS in AOT reverse micelles at different CO_2 pressures and w_0. This work focuses on how CO_2 affects dynamic behavior, microviscosity, and micropolarity of the water cores in the reverse micelles.

2. Experimental Section

Materials. CO_2 (>99.995% purity) was provided by Beijing Analytical Instrument Factory. The AOT (with 99% purity) was

* Author to whom correspondence should be addressed. Tel: 86-10-62562821. Fax. 86-10-62562821: E-mail: Hanbx@iccas.ac.cn.

10.1021/jp036681c CCC: $27.50
Published on Web 02/06/2004

purchased from Sigma. The naphthalene-based hydrophobic probe Prodan (≥98% purity, Fluka) and 8,1-ANS (97% purity, Aldrich) were used as the fluorescence probes. Isooctane (AR grade) was supplied by Beijing Chemical Plant. Double distilled water was used.

Preparation of the Probe-Containing Reverse Micelles. The reverse micellar solution was prepared by dissolving the required amount of AOT into isooctane in a glass tube, followed by adding a suitable amount of water and probes (Prodan or 8,1-ANS). The glass tube was shaken until the solution became clear. In this work, the concentrations of AOT, Prodan, and 8,1-ANS were 0.1, 5×10^{-6}, and 2×10^{-6} M in all experiments, respectively. The molar ratio of fluorophore to surfactant was very low so that no more than one probe molecule would be present per reverse micelle on an average. The low ratio made a minimal perturbation to the micellar organization and negligible inter-probe interactions possible.[46−47]

Steady-State Fluorescence Measurements. The apparatus used for the steady-state fluorescence spectroscopic measurement consisted mainly of a gas cylinder, a high-pressure pump, a fluorescence spectrophotometer (F-2100, Hitachi), and a high-pressure fluorescence sample cell. The sample cell was composed mainly of a stainless steel body with four channels, four quartz windows 3.0 cm in diameter and 0.7 cm in thick. The inner volume of the sample cell was 8.44 mL. It was thermostated to ±0.2 °C of the desired temperature by three heaters and a temperature controller. The emission spectra were measured on the spectrophotometer equipped with a computer. A Xe lamp was used as the excitation resource. No additional filters were used. The excitation wavelengths were 360 nm for Prodan and 369 nm for 8,1-ANS, respectively. Both the excitation and emission bandwidths were 5 nm.

In the experiment, the air in the sample cell was first replaced by CO_2. Then a suitable amount of reverse micellar solution was loaded into the cell. The temperature of the cell was maintained at the desired value. CO_2 was charged with the high-pressure pump until the sample cell was full. In this work, all the fluorescence experiments were conducted at pressures where the water was stable in the micellar cores, which was known from our previous phase behavior study.[45]

Time-Resolved Fluorescence Measurements. The apparatus and procedures used in the fluorescence lifetime measurement were the same as those performed in steady-state fluorescence experiment, except that the spectrophotometer was FLS 920 spectrophotometer with the single photon counting system (Edinburgh Instruments), which was operated by the F900 Software. The excitation light source was Xe900 with pulse width = 1 ns. To optimize the signal-to-noise ratio, 10 000 photo counts were collected in the peak channel. Data analysis was performed by a deconvolution method using a nonlinear least-squares fitting program with the F900 Software. The quality of the fit was estimated by the reduced χ^2 and standard deviation.[48] A fit was considered acceptable when the value of χ^2 was between 1.00 and 1.30. All fluorescence decay experiments were measured at $\lambda_{em} = 466$ nm for 8,1-ANS in all cases.

3. Results and Discussion

Prodan Emission in CO_2-Expanded Reverse Micellar Solutions. Fluorophore Prodan is a novel molecular reporter with potential added advantages for a new approach to micelle characterization. Prodan's solubility in a wide range of solvents enables the distribution of this neutral probe into multiple micellar microregions.[49−51] In reverse micelles, the partition of Prodan in different regions is governed by the noncovalent interaction such as hydrogen bonding, van der Waals or dipole forces, and hydrophobic effects.[51] Therefore, changes of the emission spectra are indicative of varied properties of local environment inside the reverse micelles. Figure 1 gives some typical spectra of Prodan in reverse micelles with $w_0 = 25$ at different CO_2 pressures. As we can see, by adding CO_2 into the reverse micelles, the emission spectra of Prodan exhibit interesting changes, i.e., the emission intensity gradually increases accompanied by a blueshifted peak around 410 nm and a redshifted peak around 495 nm.

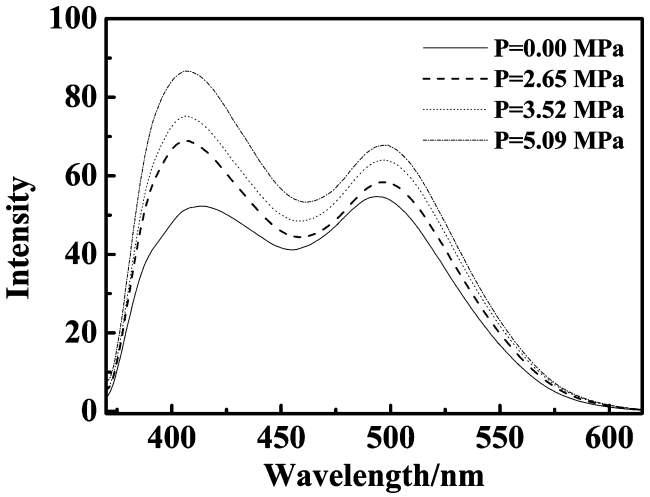

Figure 1. Fluorescence emission spectra of Prodan in AOT reverse micelles at different CO_2 pressures ($w_0 = 25$).

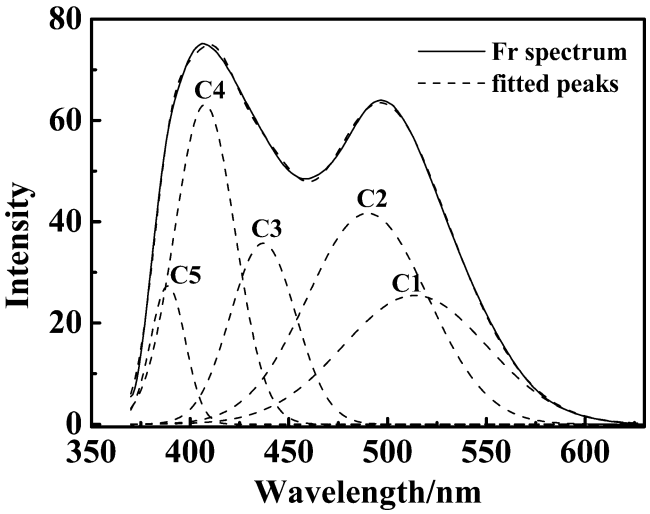

Figure 2. Resolution of Prodan emission spectrum for AOT reverse micelles with $w_0 = 25$ and CO_2 pressure of 3.52 MPa.

The Peakfit software was used to treat these emission spectra, and a sum of overlapping Gaussian functions with frequency as the independent variable was obtained. In all deconvoluted spectra, the minimum number of components is required to achieve a best fit with a minimum r^2 (random scattering of residual) of 0.999. An example of the emission peaks of Prodan in AOT reverse micelles ($w_0 = 25$, $P_{CO_2} = 3.52$ MPa) deconvoluted is illustrated in Figure 2. From the figure, it can be seen that five fluorescence emission components (C1, C2, C3, C4, and C5) with the emission maximum (λ_{em}^{max}) around 505, 488, 442, 405, and 388 nm were resolved, respectively. The observed behavior of Prodan fluorescence is consistent with the premise that Prodan partitions into multiple environments within the reverse micelles, specifically the bulk hydrocarbon continuum, the AOT interface of surfactant tails, the bound water

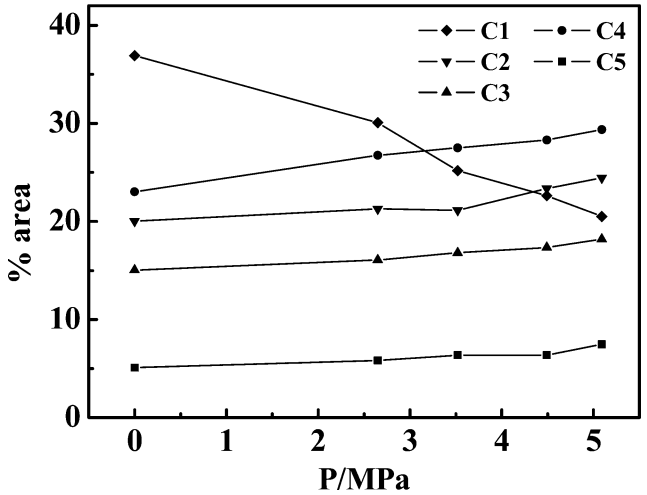

Figure 3. Effect of CO_2 pressure on % areas of Gaussian peaks of Prodan fluorescence emission in AOT reverse micelles ($w_0 = 25$).

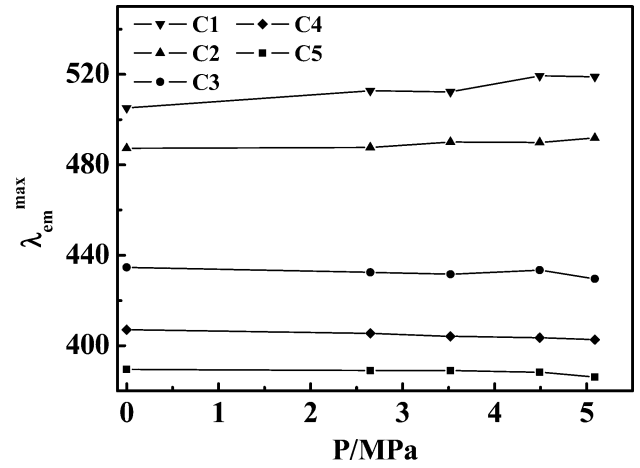

Figure 4. Effect of CO_2 pressure on λ_{em}^{max} of Prodan fluorescence emission in AOT reverse micelles ($w_0 = 25$).

interface at the AOT headgroups, and the inner bulk water pool.[49−51] A longer wavelength component with an average λ_{em}^{max} of 505 nm (C1) is associated with emission from Prodan molecules inside the "free" water pool, while those at 488 nm (C2) and 442 nm (C3) are attributed to the microregions of bound water and AOT interface of the reverse micelles, respectively. The components at 405 and 388 nm (C4 and C5) result from the probe in hydrocarbon continuum.[49−51]

The effects of pressure on the percentage contribution (% area) and λ_{em}^{max} of the Gaussian components of Prodan emission in AOT reverse micelles with $w_0 = 25$ are presented in Figures 3 and 4, respectively. In Figure 3, the percentage contribution of 505 nm (C1) decreases with increasing CO_2 pressure, while the percentage contribution of the other four components (C2, C3, C4, and C5) increases gradually with CO_2 pressure. As for the maximum emission wavelength (λ_{em}^{max}) of the components, as shown in Figure 4, an increase (10 nm) in λ_{em}^{max} of C1 and slight increase (3 nm) in λ_{em}^{max} of C2 are observed with increasing CO_2 pressure. λ_{em}^{max} of C3 is nearly independent of CO_2 pressure, while those of C4 and C5 slightly decrease with an increase in CO_2 pressure.

The change of these two parameters for each component is due to the varied environment of the Prodan. The redshift of λ_{em}^{max} for C1 shows increased polarity inside the water cores with an increase in CO_2 pressure. The decrease in percentage contribution of C1 indicates the reduced quantity of the probe

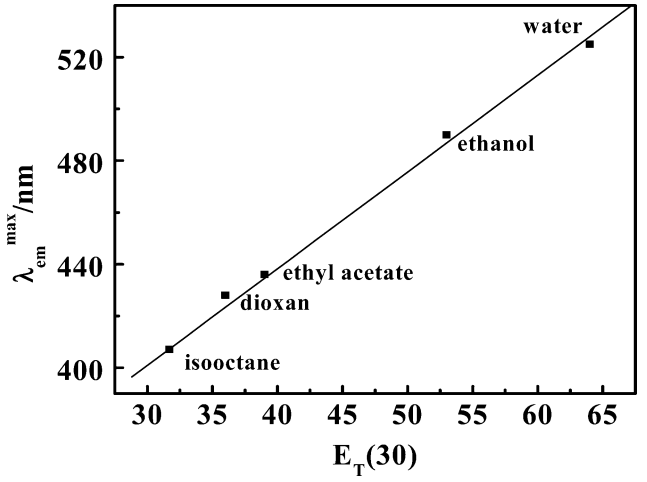

Figure 5. λ_{em}^{max} of Prodan in different solvents vs $E_T(30)$ values for fluorescence emission (λ_{ex} = 360 nm, excitation and emission bandwidths = 5 nm).

near the middle of the water cores. This may result mainly from the increased polarity of the water core with increasing pressure of CO_2 because the probe has hydrophobic groups. The redshift of λ_{em}^{max} for C2 is an indication of increased polarity of the bound water layer with the increase of CO_2 pressure. As for C3, C4, and C5, the change of λ_{em}^{max} with CO_2 pressure is not obvious. This is understandable because CO_2 is a nonpolar substance and it cannot change the polarity of nonpolar bulk regions considerably. All of the percentage contributions from C2 to C5 increase with increasing pressure. The reason is that the probe distributes in different regions and thermodynamic equilibrium is achieved as conditions are fixed. However, the equilibrium will be shifted as conditions are changed. Properties of various regions in the micellar solution are varied as pressure is increased. As discussed above, the contribution from C1 is reduced considerably, which is favorable to increase the amount of the probe in other regions. Because of the above reason, which is the relocation of Prodan from the polar to a less polar microenvironment, the 410-nm fluorescence peak is enhanced relative to the 495-nm peak upon pressure elevation. As a consequence, the total emission intensity increased. We investigated the reverse micelles with $w_0 = 5$, 10, and 15 at different CO_2 pressures, and the similar results as discussed above were also observed.

The micropolarities of micellar cores at different CO_2 pressures can be characterized by the empirical polarity parameter $E_T(30)$. By use of the empirical polarity index $E_T(30)$ (for the maximum emission around 495 nm),[50−52] the quantitative measures of polarity of the local environment of Prodan inside the CO_2-expanded AOT reverse micelles can be quantified. For this purpose, the emission maximum of Prodan in different solvents of known $E_T(30)$ values[52] was first determined in this work. These data were used to draw a calibration plot (Figure 5) from which we estimated the empirical polarity parameter $E_T(30)$ in reverse micelles of different w_0 values and at different CO_2 pressures. Figure 6 gives the obtained $E_T(30)$ values at different CO_2. It can be seen that, for all the micellar solutions with different w_0 values, $E_T(30)$ increases gradually with increasing CO_2 pressure. This results from the fact that more CO_2 is dissolved in the water cores, and therefore more HCO_3^- and H^+ are produced.[45] Moreover, as we can see from Figure 6, $E_T(30)$ values of the reverse micelles with $w_0 = 15$ and 25 are much larger and increase more significantly with pressure than that with $w_0 = 5$ and 10.

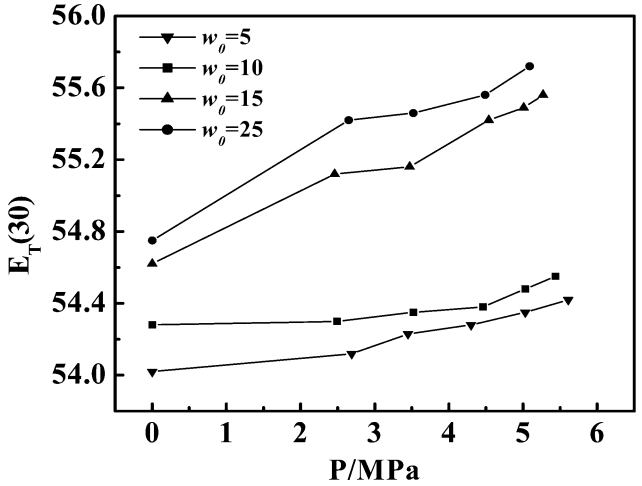

Figure 6. $E_T(30)$ values vs CO_2 pressures in AOT reverse micelles with different w_0.

The main reason is that the reverse micelles with the larger w_0 value contain more free water and more H_2CO_3 are ionized, which can increase micropolarity more efficiently.

8,1-ANS Emission in CO_2-Expanded Reverse Micellar Solutions. The basic photophysics process of 8,1-ANS has been studied extensively[30−31,53−55]. It can be expressed by the following scheme

$$S_0 \rightarrow S_{1,np} \xrightarrow{e^- \text{transfer}} S_{1,ct} \xrightarrow{e^- \text{transfer}} S_0$$
$$\downarrow \qquad\qquad \downarrow$$
$$h\nu_{F,np} \qquad h\nu_{F,ct}$$

8,1-ANS excitation leads to formation of the $S_{1,np}$ excited singlet state, which subsequently can undergo intramolecular charge transfer to form another excited singlet state $S_{1,ct}$. Emission from the state $S_{1,ct}$ is then quenched to the ground state S_0 by the nonradiative electron transfer. However, the rates of the two processes ($S_{1,np}$ to $S_{1,ct}$ and $S_{1,ct}$ to S_0) are controlled not only by the polarity of the medium but also by the viscosity of the environment of probes. The electron transfer to $S_{1,ct}$ is favored by an increased solvent dielectric relaxation, which causes a redshift in λ_{max}.[53] Emission from the $S_{1,ct}$ state is quenched by nonradiative electron transfer, and this is enhanced by increasing viscosity. Thus the quantum yield decreases with a decrease in the viscosity of the media.[32]

The steadyfluorescence spectra of 8,1-ANS in the reverse micelles with $w_0 = 2$, 5, and 10 were determined at 303.2 K and different pressures. As an example, Figure 7 gives some typical spectra of 8,1-ANS in the reverse micelles with $w_0 = 5$. As we can see, by increasing the CO_2 pressure, the intensity of the fluorescence is decreased gradually accompanied with a slight redshift. The changes of the fluorescence can be mainly attributed to the changes of the microenvironment inside the reverse micelles since 8,1-ANS mainly exists inside the reverse micelles.[30−32] It can be concluded that the increase in CO_2 pressure results in a decrease in microviscosity and increase in micropolarity of the water cores inside the reverse micelles.

Lifetime of 8,1-ANS in the Micellar Solutions. The lifetime of 8,1-ANS in the micellar cores of the reverse micelles was studied with the time-resolved fluorescence, which further gives direct information on the dynamic processes in the water pool of the reverse micelles. The time-resolved fluorescence spectra of reverse micellar solution with $w_0 = 2$, 5, and 10 were determined at 303.2 K. A representative decay curve in the water/AOT/isooctane system ($w_0 = 5$) with increasing CO_2 pressure is shown in Figure 8, from which it can be seen that the decay of the probe in reverse micelles becomes faster with an increase in CO_2 pressure. In addition, the decay is not a monoexponential from its decay trend.

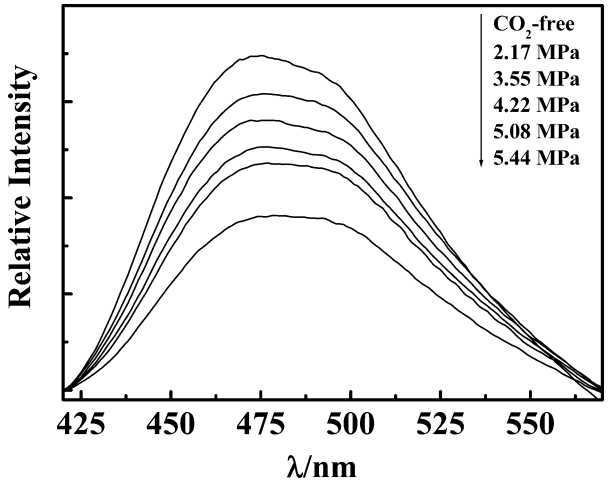

Figure 7. Emission spectra of 8,1-ANS (2×10^{-6} M) in water/AOT/isooctane reverse micelles ($T = 303.2$ K, [AOT] = 0.1 M, $w_0 = 5$) at different CO_2 pressures.

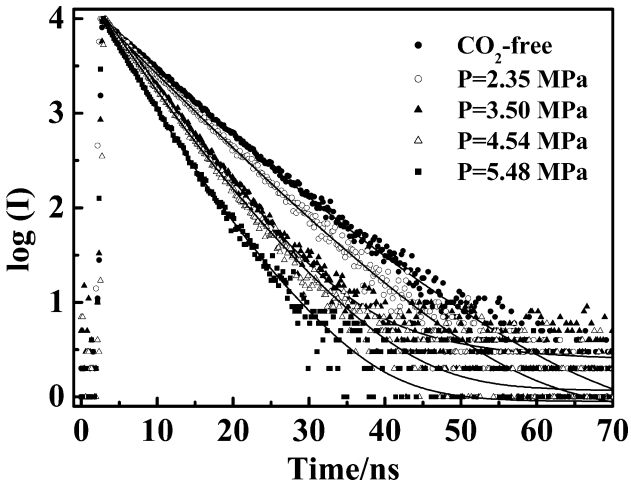

Figure 8. Fluorescence decay curves of 8,1-ANS (2×10^{-6} M) in AOT reverse micelles ([AOT] = 0.1 M, $w_0 = 5$) at 303.2 K and different CO_2 pressures. The solid curve represents the computer best fit of the experimental point.

The nonlinear least-squares fitting accompanied by deconvolution is used to treat these curves, and a biexponential decay proves to model the experimental data best with a reduced χ^2 values between 1.00 and 1.30, which is shown in Table 1. In the table, τ_1 and τ_2 are the deconvoluted lifetimes; α_1 and α_2 are the corresponding components, respectively. For a typical system, τ_1 is larger than τ_2. These two lifetimes can be attributed to different microregions of water inside the reverse micellar cores,[56−58] as the models shown in Figure 9. τ_1 corresponds to the region where the probe (denoted by the black ellipse) is associated with the head region and its mobility is restricted, as shown in model a of Figure 9; τ_2 corresponds to the probe situation near the center of the water cores, and the microenvironment is more fluid and hydrophilic than the interfacial region of the micellar cores,[56−58] which is shown as model b of Figure 9. As we can see from Table 1, τ_1 and τ_2 reduce simultaneously with increasing CO_2 pressure, which results from the increased micropolarity and decreased microviscosity of the bound and free water microregions. And it is found that τ_1 decreases faster than τ_2 with pressure, which indicates that CO_2

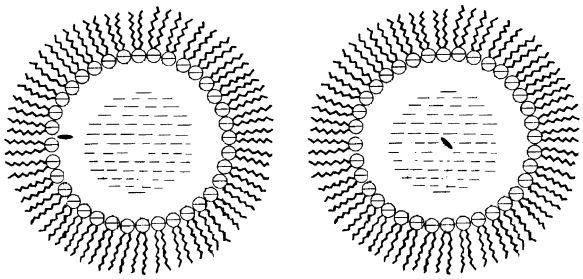

(a) (b)

Figure 9. Models for the location of 8,1-ANS bounded to the ionic headgroups of AOT surfactant (a) and located in the center of the AOT water pool (b) in the water cores of reverse micelles.

TABLE 1: Fluorescence Parameters of 8,1-ANS inside the AOT Reverse Micelles at Different Conditions ([AOT] = 0.1 M, T = 303.2 K)

w_0	P/MPa	α_1	τ_1/ns	α_2	τ_2/ns	χ^2	τ/ns
2	CO_2 free	0.53	9.33	0.47	6.35	1.115	8.22
	3.07	0.52	8.35	0.48	5.79	1.165	7.35
	3.52	0.48	7.95	0.52	5.32	1.214	6.85
	4.55	0.53	7.05	0.47	4.63	1.065	6.16
	4.97	0.60	6.89	0.40	4.46	1.018	6.16
	5.54	0.52	6.41	0.48	4.29	1.036	5.61
5	CO_2 free	0.41	7.98	0.59	5.07	1.108	6.59
	2.35	0.23	7.67	0.77	4.95	1.208	5.81
	3.50	0.07	7.38	0.93	4.08	1.145	4.47
	4.54	0.09	7.38	0.91	3.65	1.092	4.29
	4.97	0.13	5.90	0.87	3.68	1.202	4.09
	5.48	0.22	5.06	0.78	2.90	1.077	3.61
10	CO_2 free	0.06	7.81	0.94	3.28	1.193	3.85
	2.43	0.11	6.41	0.89	2.79	1.052	3.59
	3.50	0.06	5.52	0.94	2.82	1.237	3.12
3.12	4.57	0.08	5.61	0.92	2.60	1.263	3.08
3.08	5.32	0.10	5.19	0.90	2.53	1.278	3.02
3.02							

has a more obvious effect on the bound water in the micellar cores. Moreover, the component of each lifetime varies with increasing CO_2 pressure, which also results mainly from the changes in microenvironment of the water cores at different CO_2 pressures. Here we adopt a single-characteristic parameter that hopefully represents the reverse micellar system having multiexponential decay components. For this purpose, mean lifetime is calculated using the following equation[59]

$$\langle\tau\rangle = \frac{\alpha_1\tau_1^{\,2} + \alpha_2\tau_2^{\,2}}{\alpha_1\tau_1 + \alpha_2\tau_2}$$

where τ is the mean decay time. The calculated average lifetime at different pressures is shown in Table 1. It can be seen that increasing CO_2 pressure results in a decrease in τ. This essentially means that the reorganization of the water molecules in the reverse micelles becomes faster upon increasing the CO_2 pressures, which results from the increased polarity and decreased viscosity as discussed in the steady-states fluorescence spectra.

For the reverse micellar solutions with $w_0 = 2$ and 10, similar trends are observed, as shown in Table 1. It can be seen that the mean lifetime τ decreases more rapidly with a larger w_0. This is due to the increased flexibility in the larger water cores, which is similar to the results reported in AOT/water/alkene reverse micelles in the absence of CO_2.[30,60] The τ at higher pressures is smaller because CO_2 can change the polarity and viscosity of water cores.

Temperature also affects the rate of water relaxation, obviously. The results at 294.2, 303.2, and 313.2 K are listed in Table 2. The decay time of the probe inside the CO_2-free AOT reverse micelles ($w_0 = 5$) is reduced as temperature is increased, and the calculated average lifetime at these temperatures are 7.90, 6.59, and 5.93 ns, respectively. This originates mainly from the fact that the fluidity of the micelle interior is improved with increasing temperature[30−31,60]. In the presence of CO_2 (4.55 MPa), the decay time is respectively 4.70, 4.27, and 3.64 ns at the three temperatures. The relaxation rate decreases with added CO_2, which is consistent with the increased polarity and decreased viscosity as discussed above.

TABLE 2: Comparison of Fluorescence Parameters of 8,1-ANS inside the AOT Reverse Micelles at Different Temperature and Pressure (w_0 = 5)

P/MPa	T/K	α_1	τ_1/ns	α_2	τ_2/ns	χ^2	τ/ns
CO_2 free	294.2	0.69	8.59	0.31	5.49	1.186	7.90
	303.2	0.41	7.98	0.59	5.07	1.108	6.59
	313.2	0.39	7.15	0.61	4.75	1.021	5.93
4.55	294.2	0.09	7.83	0.91	4.11	1.090	4.70
4.54	303.2	0.09	7.38	0.91	3.65	1.092	4.27
4.57	313.2	0.05	6.44	0.95	3.39	1.104	3.64

4. Conclusion

The effects of compressed CO_2 on the properties and internal dynamics of water-in-isooctane microemulsions formed with AOT were investigated using fluorescence spectroscopy. The steady-state fluorescence spectroscopy with Prodan as the sovachromic probe indicates that compressed CO_2 results in an increase in micropolartity of water inside the reverse micelles. With 8,1-ANS as the fluorescent probe, a decrease in viscosity inside the micellar cores is revealed. The time-resolved fluorescence spectroscopy further demonstrates that the solvent relaxation rate in the micellar cores is increased with increased CO_2 pressure.

Acknowledgment. The authors are grateful to the National Natural Science Foundation of China (20133030) and Ministry of Science and Technology for the financial support (G2000078103).

References and Notes

(1) *Reverse Micelles*; Luisi, P. L., Straube, B. E., Eds.; Plenum Press: New York, 1984.
(2) Luisi, P. L. *Angew. Chem., Int. Ed. Engl.* **1985**, *24*, 439.
(3) Fendler, J. H. *Annu. Rev. Phys. Chem.* **1984**, *35*, 137.
(4) Ekwall, P.; Mandell, L.; Fontell, K. *J. Colloid Interface Sci.* **1970**, *33*, 215.
(5) Zulauf, M.; Eicke, H. F. *J. Phys. Chem.* **1979**, *83*, 480.
(6) Mantegazza, F.; Degiorgio, V.; Giardini, M. E.; Price, A. L.; Teutler, D. C. S.; Robinson, B. H. *Langmuir* **1998**, *14*, 1.
(7) De, T. K.; Maitra, A. *Adv. Colloid Interface Sci.* **1995**, *59*, 95.
(8) Ohde, H.; Wai, C. M.; Kim, H.; Kim, J.; Ohde, M. *J. Am. Chem. Soc.* **2002**, *124*, 4540.
(9) Ji, M.; Chen, X.; Wai, C. M.; Fulton, J. L. *J. Am. Chem. Soc.* **1999**, *121*, 2631.
(10) Holmes, J. D.; Bhargava, P. A.; Korgel, B. A.; Johnston, K. P. *Langmuir* **1999**, *15*, 6613.
(11) Vanag, V. K.; Hanazaki, I. *J. Phys. Chem.* **1996**, *100*, 10609.
(12) Correa, N. M.; Durantini, E. N.; Silber, J. J. *J. Org. Chem.* **1999**, *64*, 5757.
(13) Buriak, J. M.; Osborn, J. A. *Organometallics* **1996**, *15*, 3161.
(14) Freeman, K. S.; Tang, T. T.; Shah, R. D. E.; Kiserow, D. J.; McGown, L. B. *J. Phys. Chem. B* **2000**, 104, 9312.
(15) Martinek, K.; Levashov, A. V.; Klyachko, N.; Khmelnitski, Y. L.; Berezin, I. V. *Eur. J. Biochem.* **1986**, *155*, 453.
(16) Jain, T. K.; Varshney, M.; Maitra, A. *J. Phys. Chem.* **1989**, *93*, 7409.
(17) Bardez, E.; Nguyen, C. V. *Langmuir* **1995**, *11*, 3374.
(18) Fulton, J. L.; Pfund, D. M.; Desimone, J. M.; Capel, M. *Langmuir* **1995**, *11*, 4241.
(19) Maitra, A. *J. Phys. Chem.* **1984**, *88*, 5122.
(20) Ray, S.; Bisal, S. R.; Moulik, S. P. *Langmuir* **1994**, *10*, 2507.

(21) Wong, M.; Thomas, J. K.; Grätzel, M. *J. Am. Chem. Soc.* **1976**, *98*, 2391.
(22) Lissi, E. A.; Engel, D. *Langmuir* **1992**, *8*, 452.
(23) Hasegawa, M.; Sugimura, T.; Suzaki, Y.; Shindo, Y. *J. Phys. Chem.* **1994**, *98*, 2120.
(24) Behera, G. B.; Mishra, B. K.; Behera, P. K.; Panda, M. *Adv. Colloid Interface Sci.* **1999**, *82*, 1.
(25) Chattopadhyay, A.; Mukherjee, S.; Raghuraman, H. *J. Phys. Chem. B* **2002**, *106*, 13002.
(26) Betts, T. A.; Bright, F. V. *Appl. Spectrosc.* **1990**, *44*, 1196.
(27) Parusel, A. B. J.; Nowak, W.; Grimme, S.; Kohler, G. *J. Phys. Chem. A* **1998**, *102*, 7149.
(28) Harianawala, A. I.; Bogner, R. H. *J. Lumin.* **1998**, *79*, 97.
(29) Venables, D. S.; Huang, K.; Schmuttenmaer, C. A. *J. Phys. Chem. B* **2001**, *105*, 9132.
(30) Zhang, J.; Bright, F. V. *J. Phys. Chem.* **1991**, *95*, 7900.
(31) Zhang, J.; Bright, F. V. *J. Phys. Chem.* **1992**, *96*, 5633.
(32) Yazdi, P.; McFann, G. J.; Fox, M. A.; Johnston, K. P. *J. Phys. Chem.* **1990**, *94*, 7224.
(33) Müller, M.; Meier, U.; Kessler, A.; Mazzotti, M. *Ind. Eng. Chem. Res.* **2000**, *39*, 2260.
(34) Yates, M. Z.; Birnbaum, E. R.; McCleskey, T. M. *Langmuir* **2000**, *16*, 4757.
(35) Kendall, J. L.; Canelas, D. A.; Young, J. L.; DeSimone, J. M. *Chem. Rev.* **1999**, *99*, 543.
(36) Buhler, E.; Dobrynin, A. V.; DeSimone, J. M.; Rubinstein, M. *Macromolecules* **1998**, *31*, 7347.
(37) Park, Y. K.; Curtis, C. W.; Roberts, C. B. *Ind. Eng. Chem. Res.* **2002**, *41*, 1504.
(38) Subramaniam, B.; Rajewski, R. A.; Snavely, K. *J. Pharm. Sci.* **1997**, *86*, 885.
(39) Bungert, B.; Sadowski, G.; Arlt, W. *Ind. Eng. Chem. Res.* **1998**, *37*, 3208.
(40) Zhang, H. F.; Lu, J.; Han, B. X. *J. Supercrit. Fluids* **2001**, *20*, 65.
(41) Zhang, H. F.; Han, B. X.; Yang, G. Y.; Yan, H. K. *J. Colloid Interface Sci.* **2000**, *232*, 269.
(42) Zhang, J. L.; Han, B. X.; Liu, J. C.; Zhang, X. G.; He, J.; Liu, Z. M. *Chem. Commun.* **2001**, 2724.
(43) Zhang, J. L.; Han B. X.; Liu, J. C. *Chem.*−*Eur. J.* **2002**, *8*, 3879.
(44) Zhang, J. L.; Han, B. X.; Liu, D. X.; Dong, Z. X.; Liu, J.; Mu, T. C.; Zhao, G. Y.; Li, D.; Wang, J.; Dong, B. Z.; Zhao, H.; Rong, L. X. *J. Chem. Phys.* **2003**, *118*, 3329.
(45) Liu, D. X.; Zhang, J. L.; Han, B. X.; Fan, J. F.; Mu, T. C.; Liu, Z. M.; Wu, W. Z.; Chen, J. *J. Chem. Phys.* **2003**, *119*, 4873.
(46) Guharay, J.; Dennison, S. M.; Sengupta, P. K. *Spectrochim. Acta, Part A* **1999**, *55*, 1091.
(47) Karukstis, K. K.; Frazier, A. A.; Loftus, C. T.; Tuan, A. S. *J. Phys. Chem. B* **1998**, *102*, 8163.
(48) Lampert, R. A.; Chewter, L. A.; Phillips, D.; O'Connor, D. V.; Roberts, A. J.; Meech, S. R. *Anal. Chem.* **1983**, *55*, 68.
(49) Sengupta, B.; Guharay, J.; Sengupta, P. K. *Spectrochim. Acta, Part A* **2000**, *56*, 1433.
(50) Karukstis, K. K.; Frazier, A. A.; Martula, D. S.; Whiles, J. A. *J. Phys. Chem.* **1996**, *100*, 11133.
(51) Karukstis, K. K.; Frazier, A. A.; Loftus, C. T.; Tuan, A. S. *J. Phys. Chem. B* **1998**, *102*, 8163.
(52) Ratajczak, H.; Orville-Thomas, W. J. *Molecular Interactions*; Wiley: New York, 1982; Vol. 3.
(53) Kosower, E. M.; Kanety, H.; Dodiuk, H.; Striker, G.; Jovin, T.; Boni, H.; Huppert, D. *J. Am. Chem. Soc.* **1983**, *87*, 2479.
(54) Ebberson, T. W.; Ghiron, C. A. *J. Phys. Chem.* **1989**, *93*, 7139.
(55) Slavik, J. *Biochim. Biophys. Acta* **1982**, *1*, 694.
(56) Lang, J.; Jada, A.; Malliaris, A. *J. Phys. Chem.* **1988**, *92*, 1946.
(57) Sarkar, M.; Guharay, J.; Sengupta, P. K. *J. Photochem. Photobiol. A* **1996**, *95*, 157.
(58) Kim, J.; Lee, M. *J. Phys. Chem. A* **1999**, *103*, 3378.
(59) Lakowicz, J. R. *Principles of Fluorescence Spectroscopy*; Kluwer Plenum: New York, 1999.
(60) Zhang J.; Bright, F. V. *J. Phys. Chem.* **1992**, *96*, 9068.